energy resolution of ~4% at 662 keV. Further, the intrinsic activity of these crystals between 20 keV and 3 MeV (0.02 counts/s/cm^3) is much lower in comparison to $LaBr_3$: Ce crystals (1.24 counts/s/cm^3). As the detection sensitivity of $CeBr_3$ is at least ten times larger than $LaBr_3$: Ce at 1461 and 2615 keV as reported by Quarati *et al.*[6], determination of K and Th in meteoritic and terrestrial samples is more likely to be feasible. Future measurements will determine the sensitivity of U, Th and K using $CeBr_3$ and cooled HPGe detectors.

1. Goswami, J. N. *et al.*, High energy X–γ-ray spectrometer on the Chandrayaan-1 mission to the Moon. *J. Earth Syst. Sci.*, 2005, **114**, 733–738.
2. Milbrath, B. D., Choate, B. J., Fast, J. E., Hensley, W. K., Kouzes, R. T. and Schweppe, J. E., Comparison of $LaBr_3$: Ce and NaI(Tl) scintillators for radio-isotope identification devices. *Nucl. Instrum. Meth. Phys. Res. A*, 2007, **572**, 774–784.
3. BrilLanCe^{TM} Scintillators Performance Summary, Saint Gobain Crystals Scintillation Products Technical Note, 2009.
4. Quarati, F. *et al.*, X-ray and gamma-ray response of a $2'' \times 2''$ $LaBr_3$: Ce scintillation detector. *Nucl. Instrum. Meth. Phys. Res. A*, 2007, **574**, 115–120.
5. Shukla, A. D., Bhandari, N. and Shukla, P. N., Chemical signatures of the Permian–Triassic transitional environment in Spiti Valley, India. *Geol. Soc. Am. Spec. Pap.*, 2002, **356**, 445–453.
6. Quarati, F. G. A., Dorenbos, P., Biezen, J. van der., Owens, A., Selle, M., Parthier, L. and Schotanus, P., Scintillation and detection characteristics of high-sensitivity $CeBr_3$ gamma-ray spectrometers. *Nucl. Instrum. Meth. Phys. Res. A*, 2013, **729**, 596–604.

Received 6 May 2015; revised accepted 7 January 2016

doi: 10.18520/cs/v110/i11/2135-2138

The effect of meteorological events on sea surface height variations along the northwestern Persian Gulf

Mohammad Reza Khalilabadi*

Malek-Ashtar University of Technology, Shiraz, Iran

Analysing semi-hourly sea surface height (SSH) observed by tidal stations of the National Cartographic Center (NCC) of Iran at Bushehr and Kangan ports indicates de-tided SSH during January 2014. This analysis shows the impact of two meteorological events during 16–17 and 24–25 January 2014, when the northwestern part of the Persian Gulf was affected by them. During both occurrences, the de-tided SSHs at both stations were uniform, but the impact was larger at Bushehr and weaker at Kangan. The results show that historical NCC sea-level data would be useful for validation of numerical models which are emerging as a major tool for storm surge warning system in the Persian Gulf.

Keywords: Cyclones, meteorological events, sea surface height (SSH), surge.

THE importance and dynamics of meteorological events (e.g. storm surges) have been discussed in the literature. These are atmospheric induced variations of the sea surface height (SSH) in coastal zones, which have a range of periods between some minutes to some days. These are long waves which are similar to astronomical tides[1]. Some models and software have been designed for predicting the storm surges in coastal regions[2–4]. In spite of many benefits of these models, there are some problems: field measurements to validate the predictive numerical models are rare because the designed instrumentation for measuring normal SSH variations, such as astronomical tides, breaks down under the onslaught of abnormally high sea level during major surges[5].

The Persian Gulf is an important region in the Middle East situated at the northwest of the Indian Ocean. The importance of the Persian Gulf is due to huge quantities of oil and gas. The Gulf is surrounded by six countries (Iran, Iraq, Kuwait, Saudi Arabia, Qatar and the United Arab Emirates); Iran has the longest coastline of about 900 km. The Gulf generally is affected by tropical storms. There are several Iranian islands in the Persian Gulf. The most famous among them are Hormuz, Khark, Qeshm, Kish, Tonb-e-Kuchak, Tonb-e-Bozorg and Abu-Musa[6–9]. In this communication, sea-level variations related to atmospheric pressure and wind fields at Bushehr and Kangan ports, Iran, which are situated in the northwestern region of the Persian Gulf, have been studied.

The National Cartographic Center (NCC) of Iran has established various permanent tidal stations along the northern coastlines of the Persian Gulf and the Gulf of

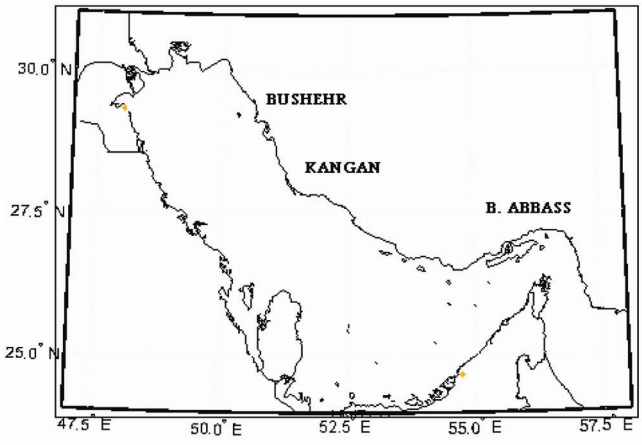

Figure 1. The study area and location of tidal stations.

*e-mail: rezakhalilabadi@gmail.com

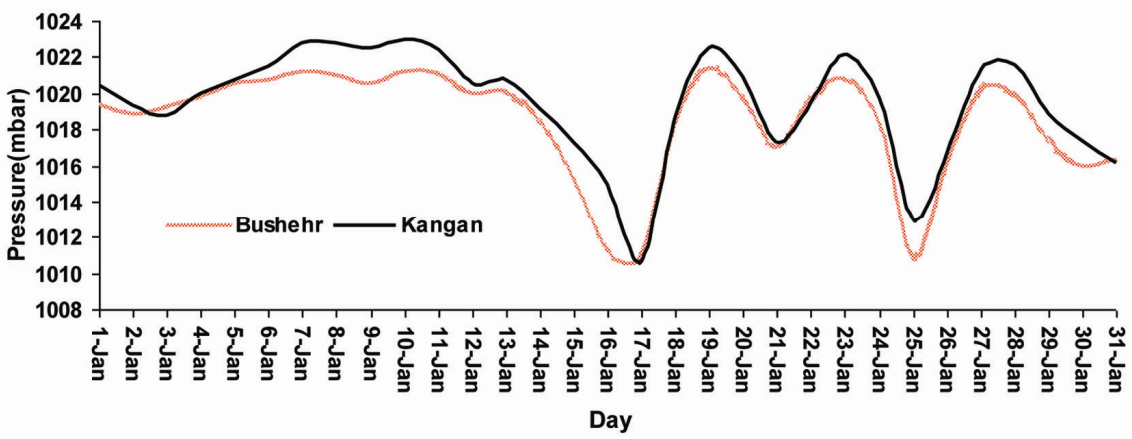

Figure 2. The barometric pressure variations at Bushehr and Kangan during January 2014.

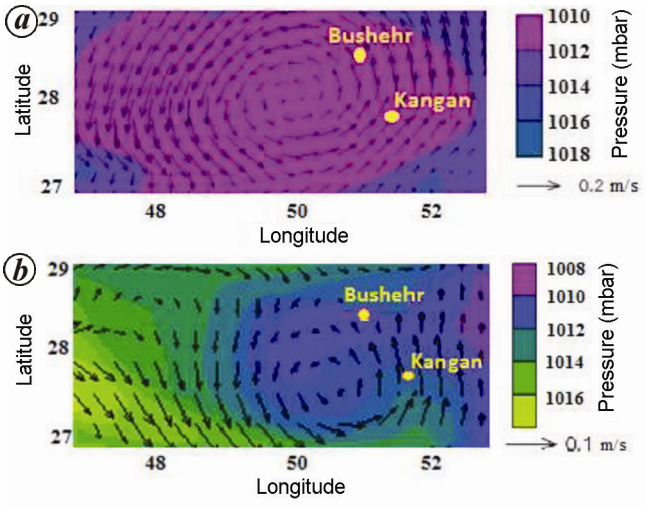

Figure 3. Average wind and pressure fields over the western part of the Persian Gulf during (***a***) 16–17 and (***b***) 24–25 January 2014.

Oman in the past 25 years[10]. Also, in recent years, several attempts have been made by the NCC to set-up temporary tidal stations for collecting water-level data which have been used for the analysis and prediction of astronomical tides in most ports and vital areas in the southern coast of Iran. The Hydrographic Department of the NCC supports a network of tide-gauges which are established at ports located along the Iranian coastline in the Persian Gulf and the Gulf of Oman. Figure 1 shows the location of these stations in the Gulf of Oman[11]. This network has been established for measuring SSH variations due to astronomical tides. These data have been used for predicting tides and extraction of surges. Predicted tides are published by the NCC in the form of annual tide tables. In this study, the NCC provided semi-hourly tide-gauge data which have been recorded during 2014 at Bushehr and Kangan ports. Figure 1 shows the locations of these ports. Also, the meteorological data during the study period were provided by the NCC and NOAA.

Analysis of the semi-hourly SSH data involves removal of the observed signal which is associated with the astronomical tide. This can be done with high accuracy because the periods of the tidal constituents are accurately known. These constituents have been defined by the motion of the Earth–Moon–Sun system[12]. The SSH oscillations related to a particular period are well known in terms of constituents for that tidal period[13]. About 60 major tidal constituents have been removed from the raw observed data. The residual signal can be associated with the impact of meteorological events, including storm surges. In our analysis, we used 62 major constituents, i.e. $N = 62$. Analysis of observed sea-level data involved using a month-long time-series of semi-hourly data of sea level as measured by a tide gauge at a tidal station. The calculated tidal signal was then subtracted from the observed data to determine the residual signal, i.e. the de-tided SSH. Some programs are available to carry out such analyses; the TASK software has been used in this study[14]. It has various steps in importing data after appropriate preparation and management of data[15]. The program has been developed by the University of British Columbia and Permanent Service for Mean Sea Level (PSMSL)[16].

This software is based on the harmonic analysis techniques. It has been developed at the National Oceanography Centre (formerly the Proudman Oceanographic Laboratory) and used throughout the world[17]. The software has been used for sea-level analysis in some marine regions such as the Bay of Bengal[5,18], Arabian Sea and Indian Ocean[19], the Persian Gulf and the Gulf of Oman[20].

The month-long historical time-series data of the de-tided SSHs have been used for detection of meteorological events. This analysis was repeated at each of the two stations on the northwest coastline, Bushehr and Kangan ports. The results identified two meteorological events during 16–17 and 24–25 January 2014, that showed the propagation of two long coastal trapped waves which moved from west to east.

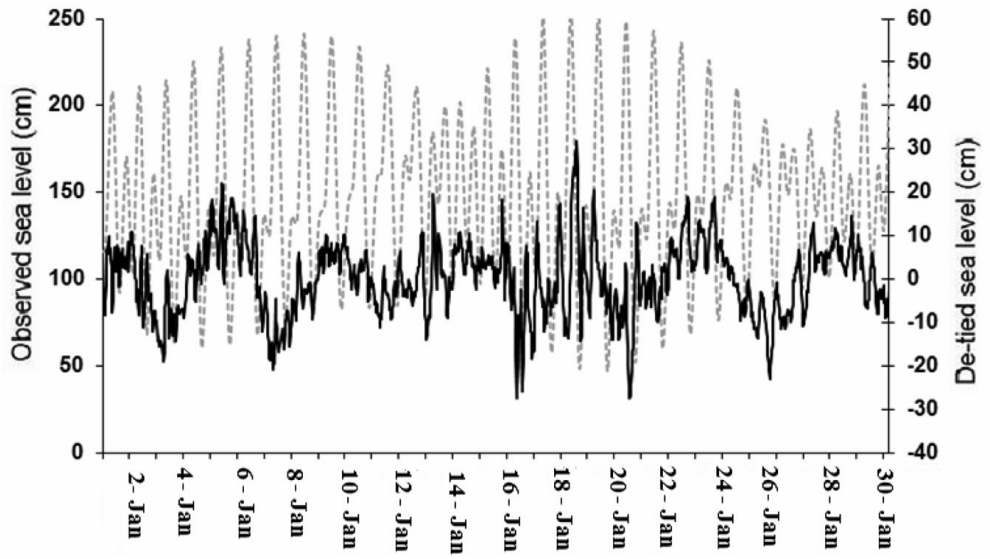

Figure 4. Observed sea level in Bushehr (dashed line) and response to the storm (bold line) during January 2014.

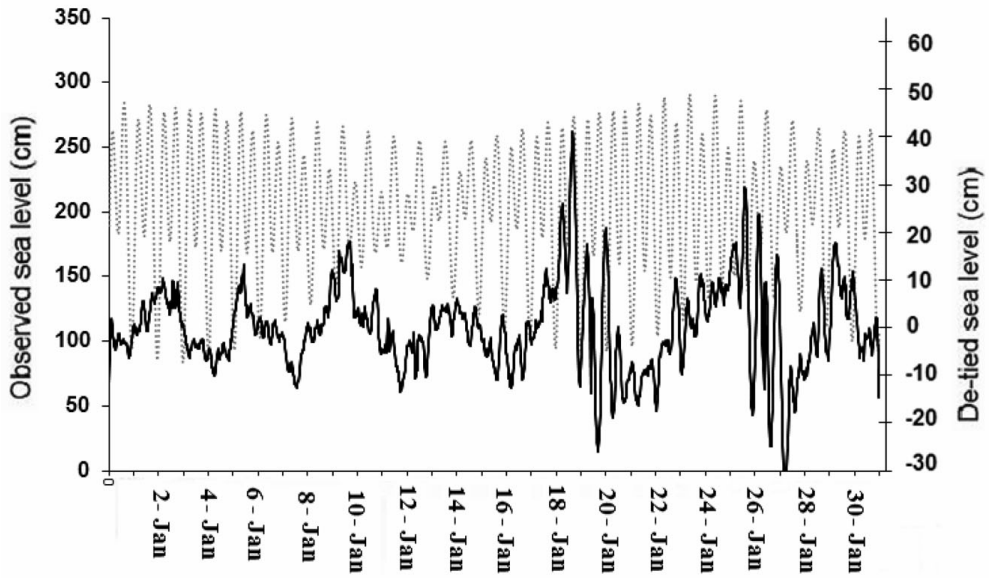

Figure 5. Observed sea level in Kangan (dashed line) and response to the storm (bold line) during January 2014.

For showing the occurrences of cyclones we used air pressure and wind field data in the study region and interpolated these data. We used inverse distance weighted (IDW) method, which estimates the value of each cell by averaging the neighborhood data values[20].

For description of meteorological events, wind and pressure fields have been illustrated. For this purpose, we used wind and pressure data in the study region. These data have been obtained from NCC and NOAA. For presentation of these fields, we used the FERRET software.

Figure 2 shows the monthly time series of atmospheric pressure for Bushehr and Kangan ports during January 2014. The figure shows two major drops in the barometric pressure on 17 and 25 January 2014.

Figure 3 *a* and *b* shows the mean wind and pressure fields over the western part of the Persian Gulf during 16–17 and 24–25 January 2014 respectively. The figure indicates the occurrence of cyclonic storms over these ports during these two periods.

Figures 4 and 5 show the effects of these two cyclonic storms on SSH variations for Bushehr and Kangan ports respectively. They also show the storm-induced SSH associated with the observed sea level. As can be seen from these figures, the observed SSHs along the south coast of Iran (in the northwestern region of the Persian Gulf) are mixed, i.e. they comprise a superposition of diurnal and semi-diurnal tidal constituents. During each month the tidal oscillation exhibits two neaps and two

spring tides. During January 2014, the spring tide occurred on 9th and the neap tide on 16th (Figures 4 and 5). Two major peaks are visible in the sea-level oscillations, one of them occurred on 15 January 2014 and the other nearly one day later. The double trough may be due to the tide–surge interaction. Throughout the cyclonic event, the atmospheric pressure at Bushehr revealed a decrease of about 10 mbar on 16 January 2014, which increased about two days later (Figure 2). Similar to Bushehr, there was a meaningful drop in atmospheric pressure at Kangan (Figure 2). While the atmospheric pressure decreased during the storm, the SSH showed an increase in Bushehr port. Such a pressure fall causes an increase in SSH close to 10 cm if the inverted barometric effect alone considered. Therefore, it is clear that in this event, the impact of wind stress is stronger than the inverted barometer effect. The rise in SSH was not limited to Bushehr port; it was also seen at Kangan port. Here the maximum increase occurred during 17 January 2014, approximately 24 h after Bushehr (Figure 5). The coastline distance between Bushehr and Kangan ports is nearly 220 km. One-day interval between these two ports infers wave celerity of about 3 m/s, which is in the category of coastally trapped wave celerity. One of the possible reasons for this is that the surge moves in the form of edge waves or shelf waves. Further studies are needed to investigate this phase change.

Figure 2 also shows a significant drop in barometric pressure in Bushehr at the end of 24 January 2014; some hours later this event occurred in Kangan. Figure 3 indicates the occurrence of a cyclonic storm over these two ports. The sea-level responses to this meteorological event have been shown in Figures 4 and 5 for Bushehr and Kangan ports respectively.

From SSH analysis it can be deduced that there are two main constituents in the Persian Gulf data. These are diurnal and semi-diurnal constituents of the tide, the latter is more important than the former. By filtering these constituents the de-tided SSH is extractable; however, in the present analysis for reliability, more than 60 tidal constituents have been considered in filtering process. The residual SSH is the influence of meteorological events over sea level.

During each meteorological event, the de-tided SSHs at both stations are uniform; however, the response at Bushehr is larger than in Kangan. The forms of de-tided SSHs follow the inverted barometer effect.

The time interval of ebb and flood along the southern coast of Iran in the Persian Gulf is nearly 6 h. Therefore, the time accuracy of surge forecasting should be shorter than this duration.

Thus, the present study showed that the meteorological impacts-induced SSH often reveals diurnal and semi-diurnal variations. This phenomenon originated from a leakage of energy from tidal to non-tidal frequencies. This may cause a minor error in the analysis. The multi-peaks in surge diagrams are the examples of this leakage which is produced by tide–surge interaction.

1. Pugh, D. T., *Tides, Surges and Mean Sea-Level*, John Wiley, Chichester, 1987.
2. Flather, R. A., A storm surge prediction model for the northern Bay of Bengal with application to the cyclone disaster in April 1991. *J. Phys. Oceanogr.*, 1994, **24**, 172–190.
3. Sindhu, B. and Unnikrishnan, A. S., Characteristics of tides in the Bay of Bengal. *Mar. Geodes*., 2013, **36**, 377–407.
4. Shija, C., Kar, S. K. and Vishal, T., Storm surge studies in the North Indian Ocean: a review. *Indian J. Geo-Mar. Sci.*, 2014, **43**(2), 125–147.
5. Sundar, D., Shankar, D. and Shetye, S. R., Sea level during storm surges as seen in tide-gauge records along the east coast of India. *Curr. Sci.*, 1999, **77**(10), 1325–1332.
6. Reynolds, R. M., Physical oceanography of the Gulf, Strait of Hormuz, and the Gulf of Oman – results from the Mt Mitchell expedition. *Pollut. Bull.*, 1993, 35–59.
7. Alessi, C. A., Hunt, H. D. and Bowe, A. S., Hydrographic data from the US Naval Oceanographic Office: Persian Gulf, Southern Red Sea, and Arabian Sea 1923–1996, Woods Hole Oceanography Institute of Technology Report, WHOI-99-02, Woods Hole Oceanographic Institution, Woods Hole, 1999.
8. Swift, S. A. and Bower, A. S., Formation and circulation of dense water in the Persian Gulf. *Geophys. Res.*,. 2003, **108**(C1), 4-1–4-21.
9. Jochen, K. and Masoud, S., The circulation of the Persian Gulf: a numerical study. *Ocean Sci.*, 2006, **2**, 27–41.
10. NCC Tidal chart manual, National Cartographic Center (NCC) of Iran, Tehran, 2015.
11. Jones, M. T. Centenary edition of the GEBCO digital atlas, British Oceanographic Data Centre, Liverpool, 2003.
12. Gill, A., *Atmosphere–Ocean Dynamices*, Academic Press, New York, 1982, pp. 662.
13. Holton, J. R., *An Introduction to Dynamic Meteorology*, Elsevier, Burlington, 2004.
14. Murray, M. T., A general method for the analysis of hourly heights of the tide. *Int. Hydrogr. Rev.*, 1964, **41**(2), 91–101.
15. Bell, C., Vassie, J. M. and Woodworth, P. L., Manual of POL/PSMSL Tidal Analysis Software Kit 2000 (TASK-2000), Proudman Oceanographic Laboratory, Merseyside, 2000.
16. Charles, M., Tidal analysis and prediction in the western Indian Ocean. Western Indian Ocean Marine Science Association and Intergovermental Oceanographic Commission (of UNESCO), 2009.
17. The National Oceanography Centre, 2015; http://noc.ac.uk/science-technology/research-groups (accessed on 26 August 2015).
18. Kumar, V., Kumar, S., Ashok, K. and Pednekar, P., Observation of oceanographic parameters of nearshore waters off Yanam during the cyclonic storm. *Curr. Sci.*, 2008, 1503–1508.
19. Jineesh, V. K. *et al.*, Mesoscale process-induced variation of the West India Coastal Current during the winter monsoon. *Environ. Monit. Assess.*, 2015, **187**, 1–13.
20. Khalilabadi, M. R. and Darius, M., The effect of super cyclone 'GONU' on sea level variation along Iranian coastlines. *Indian J. Geo-Mar. Sci.*, 2013 (in press).

Received 3 September 2015; revised accepted 24 November 2015

doi: 10.18520/cs/v110/i11/2138-2141